Design of Narrow-Bandgap Polymers. Syntheses and Properties of Monomers and Polymers Containing Aromatic-Donor and *o*-Quinoid-Acceptor Units

Chitoshi Kitamura, Shoji Tanaka, and Yoshiro Yamashita*

Department of Structural Molecular Science, The Graduate University for Advanced Studies, and Institute for Molecular Science, Myodaiji, Okazaki 444, Japan

Received October 5, 1995. Revised Manuscript Received December 6, 1995[⊗]

A series of novel monomers and polymers containing aromatic-donor and *o*-quinoid-acceptor units was prepared, and the relationship between their spectral and electrochemical properties and their structures was investigated. X-ray structure analyses of the monomers possessing thiophene units revealed coplanar conformations, whereas calculations of the monomers containing *N*-methylpyrrole showed torsional conformations. Cyclic voltammetry showed amphoteric properties for all the monomers and p- and n-doping processes for most of the polymers. The reduction potentials were primarily dependent on the electron-accepting character of the *o*-quinoid-acceptor units. The electrochemical behavior of the polymers was characterized by cyclic voltammetry and suggested narrow-bandgap systems. The bandgaps determined from optical absorption spectra range from 0.5 to 1.4 eV. The polymer composed of thiophenes and benzo[1,2-*c*;3,4-*c*′]bis[1,2,5]thiadiazole exhibited the narrowest bandgap.

Introduction

Recently, π-conjugated polymers have attracted much attention due to their characteristic electronic and optical properties.[1] In the field of materials science, band structure engineering has become important since the bandgap (E_g) is one of the most important factors of controlling physical properties. Especially, the search for polymers that possess narrow bandgaps is a current topic because such polymers are expected to be promising candidates for intrinsic organic conductors and nonlinear optical devices.[1,2] The discovery of polybenzo[*c*]thiophene whose bandgap (E_g = 1.1 eV)[3] is about 1 eV lower than that of polythiophene showed a possibility of tuning the bandgap by structural modification. Since then, much effort has been devoted theoretically[4−14] and experimentally[15−27] in order to explore the correlation between the structures and bandgaps of polymers and to further reduce bandgaps. Early, the importance of quinoid character along the polymer backbone was pointed out[4] and supported by NMR investigations.[11] Recently, several powerful approaches on the construction of narrow-bandgap systems have been suggested. One is the copolymerization of aromatic and *o*-quinoid units,[10a] indicating that the combination of monomer segments with different electronic structures can lower the bandgap through the relaxation of bond-length alternation. Another is the alternation of strong electron-donating and electron-accepting moieties,[22] showing

[⊗] Abstract published in *Advance ACS Abstracts,* January 15, 1996.

(1) For reviews, see: (a) Skotheim, T. A., Ed. *Handbook of Conducting Polymers*; Marcel Dekker: New York, 1986. (b) Patil, A. O.; Heeger, A. J.; Wuld, F. *Chem. Rev.* **1988**, *88*, 183. (c) Scherf, U.; Müllen, K. *Synthesis* **1992**, 23. (d) Brédas, J.-L., Silbey, R., Eds. *Conjugated Polymers*; Kluwer Academic Publishers: Dordrecht, 1991. (e) Roncali, J. *Chem. Rev.* **1992**, *92*, 711.

(2) (a) Nalwa, H. S. *Adv. Mater.* **1993**, *5*, 341. (b) Brédas, J.-L. *Adv. Mater.* **1995**, *7*, 263.

(3) (a) Wudl, F.; Kobayshi, M.; Heeger, A. J. *J. Org. Chem.* **1984**, *49*, 3382. (b) Kobayashi, M.; Colaneri, M. Boysel, M.; Wudl, F.; Heeger, A. J. *J. Chem. Phys.* **1985**, *82*, 5717.

(4) (a) Brédas, J.-L. *J. Chem. Phys.* **1985**, *82*, 3808. (b) Brédas, J.-L. *Synth. Met.* **1987**, *17*, 115.

(5) (a) Kertesz, M.; Lee, Y.-S. *J. Phys. Chem.* **1987**, *91*, 2690. (b) Toussaint, J. M.; Thémans, B.; André, J. M.; Brédas, J.-L. *Synth. Met.* **1989**, *28*, C205.

(6) Pranata, J.; Grubbs, R. H.; Dougherty, D. A. *J. Am. Chem. Soc.* **1988**, *110*, 3430.

(7) (a) Kertesz, M.; Lee, Y.-K. *Synth. Met.* **1989**, *28*, C545. (b) Lee, Y.-S.; Kertesz, M.; Elsenbaumer, R. L. *Chem. Mater.* **1990**, *2*. 526. (c) Otto, P.; Ladik, J. *Synth. Met.* **1990**, *36*, 327. (d) Surján, P. R.; Németh, K. *Synth. Met.* **1993**, *55−57*, 4260.

(8) Tanaka, K.; Wang, S.; Yamabe, T. *Synth. Met.* **1989**, *30*, 57.

(9) Nayak, K.; Marynick, D. S. *Macromolecules* **1990**, *23*, 2237.

(10) (a) Kürti, J.; Surján, P. R.; Kertesz, M. *J. Am. Chem. Soc.* **1991**, *113*, 9865. (b) Kürti, J.; Surján, P. R.; Kertesz, M. *Synth. Met.* **1992**, *49−50*, 537. (c) Toussaint, J. M.; Brédas, J.-L. *Macromolecules* **1993**, *26*, 5240. (d) Kürti, J.; Surján, P. R.; Kertesz, M.; Frapper, G. *Synth. Met.* **1993**, *55−57*, 4338.

(11) Hoogmartens, I.; Adriaensens, P.; Vanderzande, D.; Gelan, J.; Quattrocchi, C.; Lazzaroni, R.; Brédas, J.-L. *Macromelecules* **1992**, *25*, 7347.

(12) Toussaint, J. M.; Brédas, J.-L. *Synth. Met.* **1995**, *69*, 637.

(13) Kertesz, M. *Synth. Met.* **1995**, *69*, 641.

(14) Brocks, G. *J. Chem. Phys.* **1995**, *102*, 2522.

(15) Jenekhe, S. A. *Nature* **1986**, *322*, 345.

(16) Taliani, C.; Ruani, G.; Zamboni, R.; Bolognesi, A.; Catellani, M.; Destri, S.; Porzio, W.; Ostoja, P. *Synth. Met.* **1989**, *28*, C507.

(17) Ikenoue, Y. *Synth. Met.* **1990**, *35*, 263.

(18) Ikenoue, Y.; Wudl, F.; Heeger, A. J. *Synth. Met.* **1991**, *40*, 1.

(19) (a) Ferraris, J. P.; Lambert, T. L. *J. Chem. Soc., Chem. Commun.* **1991**, 1268. (b) Musmanni, S.; Ferraris, J. P. *J. Chem. Soc., Chem. Commun.* **1993**, 172. (c) Ferraris, J. P.; Bravo, A.; Kim, W.; Hrncir, D. C. *J. Chem. Soc., Chem. Commun.* **1994**, 991.

(20) (a) Pomerantz, M.; Chaloner-Gill, B.; Harding, L. O.; Tseng, J. J.; Pomerantz, W. J. *J. Chem. Soc., Chem. Commun.* **1992**, 1672. (b) Pomerantz, M.; Chaloner-Gill, B.; Harding, L. O.; Tseng, J. J.; Pomerantz, W. J. *Synth. Met.* **1993**, *55−57*, 960.

(21) (a) Hanack, M.; Mangold, K.-M.; Rörig, U.; Maichle-Mössmer, C. *Synth. Met.* **1993**, *60*, 199. (b) Hanack, M.; Schmid, U.; Röhrig, U.; Toussaint, J.-M.; Adant, C.; Brédas, J.-L. *Chem. Ber.* **1993**, *126*, 1487.

(22) (a) Havinga, E. E.; ten Hoeve, W.; Wynberg, H. *Polym. Bull.* **1992**, *29*, 119. (b) Havinga, E. E.; ten Hoeve, W.; Wynberg, H. *Synth. Met.* **1993**, *55−57*, 299.

(23) Lakshmikantham, M. V.; Lorcy, D.; Scordilis-Kelley, C.; Wu, X.-L.; Parakka, J. P.; Metzger, R. M.; Cava, M. P. *Adv. Mater.* **1993**, *5*, 723.

(24) (a) Tanaka, S.; Yamashita, Y. *Synth. Met.* **1993**, *55−57*, 1251. (b) Tanaka, S.; Yamashita, Y. *Synth. Met.* **1995**, *69*, 599.

(25) Preliminary communication: Kitamura, C.; Tanaka, S.; Yamashita, Y. *J. Chem. Soc., Chem. Commun.* **1994**, 1585.

(26) Preliminary communication: Karikomi, M.; Kitamura, C.; Tanaka, S.; Yamashita, Y. *J. Am. Chem. Soc.* **1995**, *117*, 6791.

(27) Preliminary communication: Kitamura, C.; Tanaka, S.; Yamashita, Y. *Chem. Lett.*, in press.

0897-4756/96/2808-0570$12.00/0

Chart 1

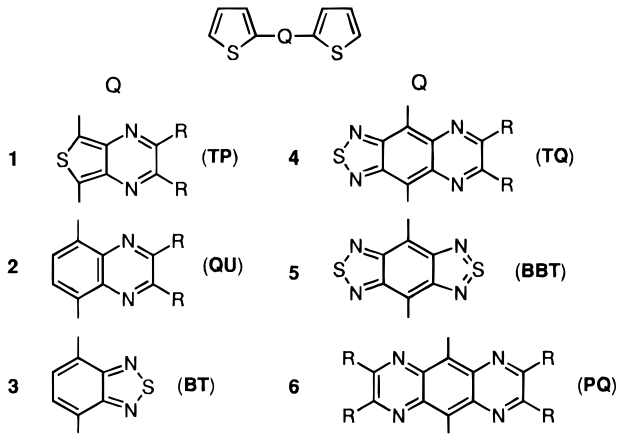

Chart 2

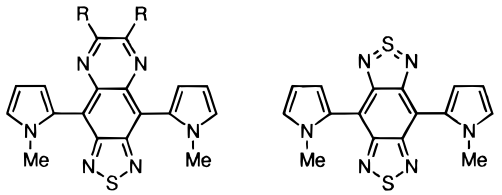

that the mixing of monomer segments with higher HOMO and lower LUMO is effective to reduce the bandgap due to the intrachain charge transfer. Moreover, the steric interaction between adjacent units relating to coplanarity should be taken into account in order to maximize the effective π-conjugation length along the polymer backbone.[9] On the basis of these guidelines, we have designed new narrow-bandgap systems, symbolized as $[-A-Q-A-]_n$, where A is a kind of aromatic-donor unit and Q is a kind of *o*-quinoid-acceptor unit. The properties of polymers are considered to correlate straightforwardly to those of structurally defined monomers [A−Q−A]. Therefore, it is important to examine the properties of monomers in detail. We have actually synthesized various new monomers **1**−**6** (Chart 1) which consist of thiophene as aromatic-donor and 10π- or 14π-electron-heterocycles as *o*-quinoid-acceptor {thieno[3,4-*b*]pyrazine (**TP**), quinoxaline (**QU**), 2,1,3-benzothiadiazole (**BT**), [1,2,5]thiadiazolo[3,4-*g*]quinoxaline (**TQ**), benzo[1,2-*c*;3,4-*c*′]bis[1,2,5]-thiadiazole (**BBT**), and pyrazino[2,3-*g*]quinoxaline (**PQ**)}. It is interesting to know to what extent the various *o*-quinoid-acceptor segments would module physical properties. These *o*-quinoid-acceptor units have no hydrogen atom at peripheral positions. Therefore, they have an advantage with no or less steric hindrance between adjacent rings when compared with benzo[*c*]-thiophene.[19b] We have also synthesized *N*-methylpyrrole derivatives **7** and **8** (Chart 2) to change the HOMO level of aromatic-donor unit. As to **1**, **2**, **4**, and **7**, some alkyl groups with different chain lengths were introduced to improve solubility. The corresponding polymers were prepared by an electrochemical method. In this paper, we describe investigations of the spectral and electrochemical properties of a series of monomers and their polymers to examine the structure−property correlation. We also present here one of the narrowest-bandgap polymers reported so far.[22,24b]

Table 1. HOMO and LUMO Energies for Some Heterocycles Calculated by the PM3 Method

heterocycle	HOMO/eV	LUMO/eV
thiophene	−9.54	−0.19
pyrrole	−8.93	1.11
N-methylpyrrole	−8.87	1.08
TP	−9.45	−1.41
QU	−9.58	−0.90
BT	−9.63	−1.81
TQ	−9.27	−2.39
BBT	−8.73	−3.21
PQ	−9.33	−1.60

Scheme 1

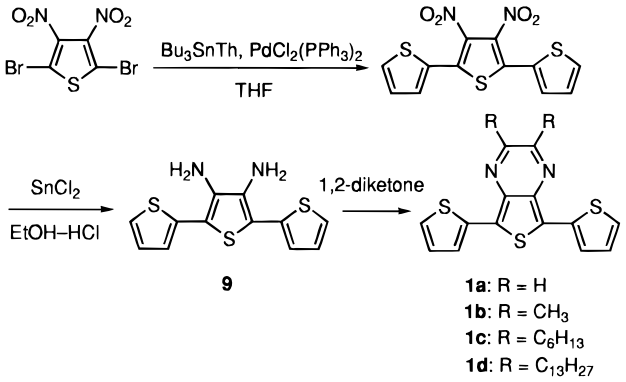

Results and Discussion

Molecular Orbital Calculations. The MNDO-PM3 calculations[28] were performed in order to estimate properties of monomers and polymers and facilitate discussion later. HOMO and LUMO energies of relating heterocycle segments are shown in Table 1. The HOMO energies of *o*-quinoid-acceptor heterocycles except for **BBT** (−8.73 eV) range from −9.63 to −9.33 eV, while their LUMO energies are in a wide range of −3.21 to −0.90 eV. Namely, the structures of *o*-quinoid-acceptor heterocycles affect primarily the LUMO levels. Among the heterocycles, therefore, using **BBT** that has the lowest LUMO is the most favorable for making the HOMO−LUMO separation small. On the other hand, the HOMO level of *N*-methylpyrrole (−8.87 eV) is higher than that of thiophene (−9.54 eV). This fact suggests that mixing of *N*-methylpyrrole and *o*-quinoid-acceptor heterocycles can lead to smaller HOMO−LUMO separation.

Syntheses of Monomers. The synthesis of monomers **1** is described in Scheme 1.[25] The Stille coupling reaction[29] of 2,5-dibromo-3,4-dinitrothiophene[30] with tributyl(thien-2-yl)stannane[31] in the presence of catalytic bis(triphenylphosphine)dichloropalladium(II) [$PdCl_2(PPh_3)_2$][32] gave a dinitro compound in 60% yield. In recent years, this type of reaction has been generally used for the syntheses of various heteroaromatic oligomers.[33] Reduction of the nitro compound with $SnCl_2$ in ethanol−hydrochloric acid produced diamine **9** in 62% yield. Condensation of **9** with 1, 2-diketones[34,35] (involv-

(28) Steward, J. J. P. *J. Comput. Chem.* **1989**, *10*, 209, 221.
(29) (a) Stille, J. K. *Angew. Chem., Int. Ed. Engl.* **1986**, *25*, 508. (b) Mitchell, T. N. *Synthesis* **1992**, 803.
(30) Mozingo, R.; Harris, S. A.; Wolf, D. E.; Hoffhine, C. E., Jr.; Eaton, N. R.; Folkers, K. *J. Am. Chem. Soc.* **1945**, *67*, 2092.
(31) Pinhey, J. T.; Roche, E. G. *J. Chem. Soc., Perkin Trans. 1* **1988**, 2415.
(32) Bailey, T. R. *Tetrahedron Lett.* **1986**, *27*, 4407.
(33) Gronowitz, S.; Peters, D. *Heterocycles* **1990**, *30*, 645.
(34) Srinivasan, N. S.; Lee, D. G. *J. Org. Chem.* **1979**, *44*, 1574.

Scheme 2

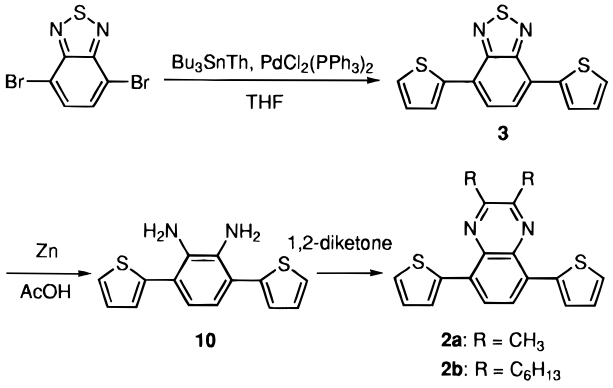

Scheme 3

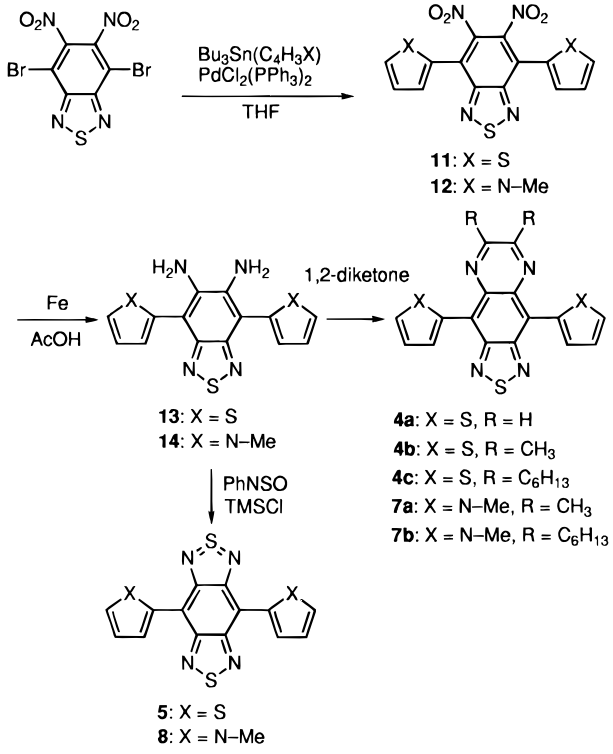

ing a synthetic equivalent of glyoxal)[36] produced **TP** derivatives **1** in 52−85% yields.

Scheme 2 shows the syntheses of monomers **2** and **3**. The coupling reaction of 4,7-dibromo-2,1,3-benzothiadiazole[37] and tributyl(thien-2-yl)stannane in the presence of $PdCl_2(PPh_3)_2$ afforded **BT** derivative **3** in 82% yield. Reduction of **3** with zinc in acetic acid accompanied by opening of the thiadiazole ring gave diamine **10** in 60% yield. **QU** derivatives **2** were prepared by condensation of **10** with 1,2-diketones in 89−90% yields.

In Scheme 3, the syntheses of monomers **4**, **5**, **7**, and **8** are described.[26,27] The coupling reaction of 4,7-dibromo-5,6-dinitro-2,1,3-benzothiadiazole[38] with tributylstannane compounds[31,39] gave dinitro compounds **11**

Scheme 4

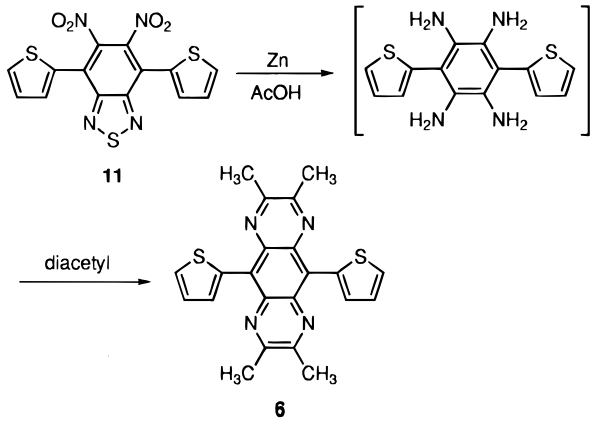

and **12**. Subsequently, reduction of **11** and **12** with iron in acetic acid yielded diamines **13** and **14** in 27% and 73% two-step yields, respectively. The condensation of **13** with 1,2-diketones gave **TQ** derivatives **4** in 50−82% yields. Similarly, the condensation of **14** with 1,2-diketones afforded **TQ** derivatives **7** in 59−62% yields. Reaction of diamines **13** and **14** with *N*-sulfinylaniline and chlorotrimethylsilane in pyridine gave **BBT** derivatives **5** and **8**, which have a stable nonclassical structure,[40] in 82 and 28% yields, respectively.

Monomer **6** was synthesized as shown in Scheme 4. Reduction of **11** with zinc in acetic acid followed by reaction of diacetyl in one pot afforded **PQ** derivative **6** in 53% yield.

In preparation of **2**, **6**, and **7**, treatment of diamines with 40% glyoxal or 1,4-dioxane-2,3-diol was unsuccessful in giving the parent pyrazine derivatives. Solubility of **4a**, **4b**, **5**, and **6** against organic solvents (even chloroform and tetrahydrofuran) was low. In contrast, solubility of *N*-methylpyrrole derivatives **7a** and **8** was high.

Properties of Monomers. The molecular structures of monomers (**1b**, **2a**, **4c**, and **5**) are shown in Figure 1. The X-ray analyses revealed that the molecules have almost planar conformations.[41] The dihedral angles between thiophene and *o*-quinoid-acceptor heterocycles were 6.5 and 11.6° for **1b**, 11.7 and 3.2° for **2a**, and 9.9 and 8.6° for **4c**, respectively. In the case of **5**, the dihedral angles were 0°. These planar conformations would certainly lead to a higher degree of π-electron delocalization.

Physical data of monomers are summarized in Table 2. The electronic spectra of monomers **1**−**8** cover almost all visible regions: **1**, red (λ_{max}, 500−529 nm); **2**, fluorescent yellow (405−407 nm); **3**, orange (466 nm); **4**, blue (591−604 nm); **5**, blue (702 nm); **6**, red (491 nm); **7**, bluish purple (571−572 nm); and **8**, blue (694 nm). Monomer **5** has the longest absorption band among the monomers, indicating the smallest HOMO−LUMO separation. Monomer **8** displays 8 nm blue shift compared to **BBT** analogue **5**, and monomers **7** exhibit about 20−30 nm blue shifts compared with **TQ** analogues **4**. These results are contrary to the initial expectation that the more electron-donating pyrrole derivatives have smaller HOMO−LUMO separation than the corre-

(35) Khalique, A. *Sci. Res.* **1967**, *4*, 129.
(36) Venuti, M. C. *Synthesis* **1982**, 61.
(37) Pilgram, K.; Zupan, M.; Skiles, R. *J. Heterocycl. Chem.* **1970**, *7*, 629.
(38) Uno, T.; Takagi, K.; Tomoeda, M. *Chem. Pharm. Bull.* **1980**, *28*, 1909.
(39) Yamamoto, M.; Izuoka, H.; Saiki, M.; Yamada, K. *J. Chem. Soc., Chem. Commun.* **1988**, 560.
(40) Ono, K.; Tanaka, S.; Yamashita, Y. *Angew. Chem., Int. Ed. Engl.* **1994**, *33*, 1977.
(41) The geometrical parameters of the thiophene rings are less reliable because of 180°-rotational disorder.

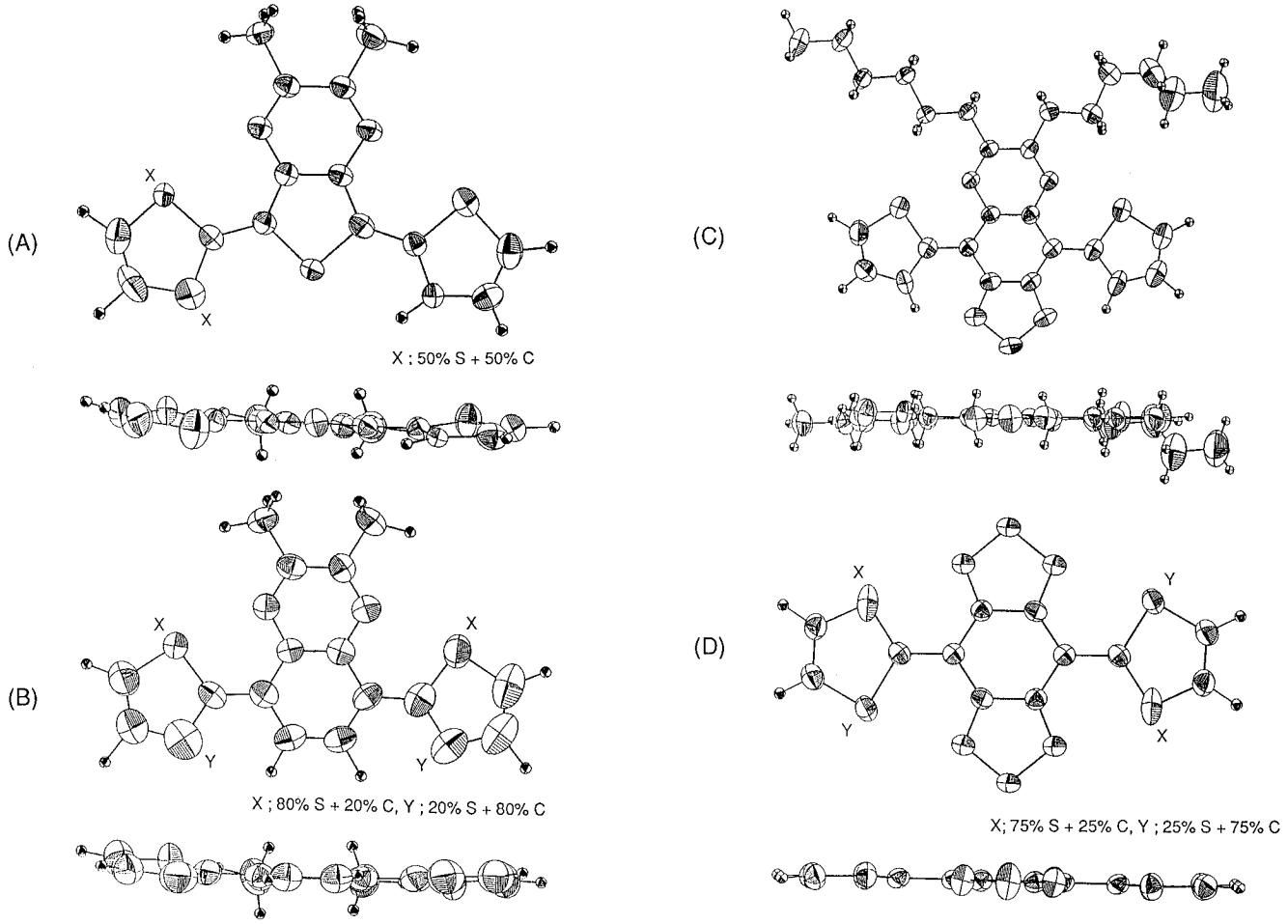

Figure 1. Molecular structures of (A) **1b**, (B) **2a**, (C) **4c**, and (D) **5**.

Table 2. Properties of Monomers

monomer	class	λ_{max}/nm (eV)[a]	E_{pa}/V[b]	E_{pc}/V[b]	$E_{pa} - E_{pc}$/V
1a	TP	529(2.35)	0.97	−1.05	2.02
1b	TP	500(2.48)	0.88	−1.36	2.24
1c	TP	502(2.48)	0.91	−1.37	2.28
1d	TP	500(2.48)	0.86	−1.37	2.23
2a	QU	405(3.06)	1.15	−1.51	2.66
2b	QU	407(3.05)	1.18	−1.49	2.67
3	BT	466(2.66)	1.23	−1.22	2.45
4a	TQ	604(2.05)	0.98	−0.72	1.80
4b	TQ	591(2.10)	1.04	−0.85	1.89
4c	TQ	593(2.09)	1.05	−0.81	1.86
5	BBT	702(1.77)	0.95	−0.53	1.48
6	PQ	491(2.53)	1.02	−1.17	2.19
7a	TQ	572(2.17)	0.86	−1.03	1.89
7b	TQ	571(2.17)	0.88	−0.99	1.87
8	BBT	694(1.79)	0.78	−0.69	1.47

[a] In $CHCl_3$. [b] 0.1 mol dm^{-3} *n*-Bu_4NClO_4 in PhCN, Pt electrode, scan rate 100 mV s^{-1}, V vs SCE.

sponding thiophene ones. Although we thought of simply mixing the segments in monomers **7** and **8**, we should have considered steric interactions. The geometry optimization of **7** and **8** by the PM3 method showed about 70° torsion structures due to the steric repulsion between the *o*-quinoid-acceptor heterocycles and the methyl group. The conformations result in the reduction of π-conjugation. To overcome this steric hindrance, the substitution of free pyrrole for *N*-methylpyrrole seems likely. Work along this line is now in progress.

Cyclic voltammetry (CV) measurements on monomers **1**−**8** were performed using a Pt disk as a working electrode in PhCN with 0.1 mol dm^{-3} *n*-Bu_4NClO_4 as the supporting electrolyte. Their cyclic voltammograms (CVs) showed both an irreversible oxidation wave and a reversible or quasi-reversible reduction wave, demonstrating an amphoteric redox property. The redox peak potentials are listed in Table 2. The oxidation peak potentials E_{pa} of the series of monomers vary from 0.78 to 1.23 V vs SCE, whereas the reduction peak potentials E_{pc} are in a wide range of −0.53 to −1.51 V. The reduction potentials reflect the LUMO levels of the *o*-quinoid-acceptor heterocycles. **BBT** derivative **5** exhibits the highest electron-accepting ability among them. On the other hand, the oxidation peak potentials of *N*-methylpyrrole derivatives **7** and **8** (0.78−0.86 V) are observed at lower potentials than those of thiophene derivatives **1**−**6** (0.86−1.23 V), showing that *N*-methylpyrrole has a slightly higher electron-donating ability than thiophene. The difference in redox potentials ($E_{pa} - E_{pc}$) approximately corresponds to the HOMO−LUMO separation determined by the absorption maxima. These results indicate that the introduction of stronger *o*-quinoid-acceptor heterocycle segment is favorable for reducing HOMO−LUMO separation.

Syntheses of Polymers. Polymers were prepared by repetitive potential-sweep anodic oxidation of the corresponding monomers **1**−**8** onto Pt disk or indium tin oxide (ITO) coated glass electrodes in PhCN containing 0.1 mol dm^{-3} *n*-Bu_4NClO_4 (for **5**, *n*-Bu_4NBF_4) at a scan rate of 100 mV s^{-1}. For **1a**, **2a**, **3**, and **7**, MeCN was also used. The polymerization smoothly occurred except for **5** and **6** whose polymerization needed a

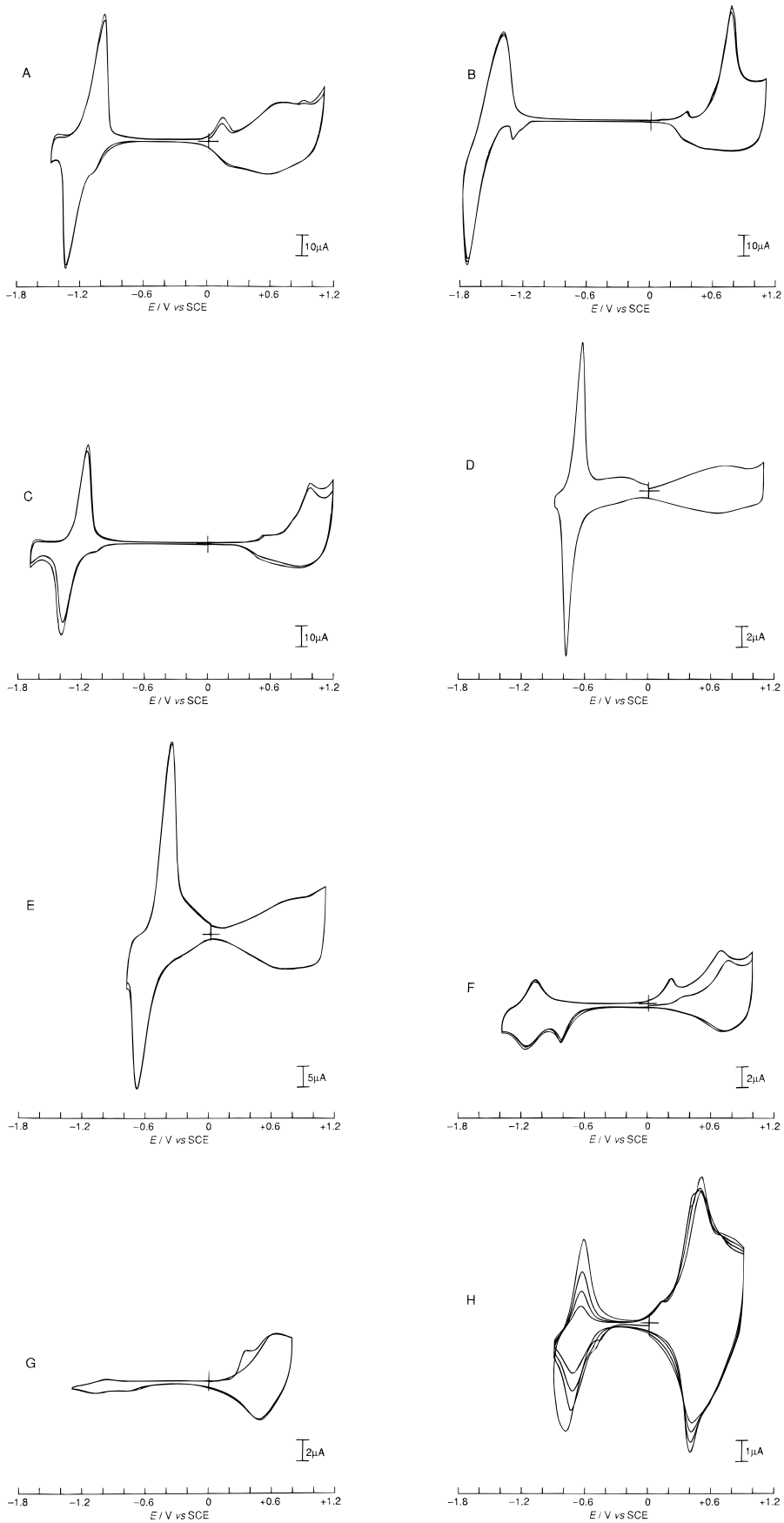

Figure 2. Cyclic voltammograms of polymers coated on Pt electrodes in PhCN containing 0.1 mol dm^{-3} *n*-Bu_4NClO_4 (for **5**, *n*-Bu_4NBF_4) at a scan rate of 10 mV s^{-1}: (A) poly-**1a**, (B) poly-**2a**, (C) poly-**3**, (D) poly-**4a**, (E) poly-**5**, (F) poly-**6**, (G) poly-**7a**, and (H) poly-**8**.

prolonged time (3−4 h) due to a low efficiency. All the polymers were obtained as insoluble deposits even if long alkyl chains were introduced as in **1**, **2**, **4**, and **7**. Electrochemical reduction of the resulting polymers

Table 3. Properties of Polymers

polymer	E_{pc}/V[a]	E_g^{opt}/eV[b]
poly-**1a**	−1.33	1.0
poly-**2a**	−1.74	1.4
poly-**3**	−1.38	1.2
poly-**4a**	−0.78	0.7
poly-**5**	−0.68	0.5
poly-**6**	−1.19	0.9
poly-**7a**		0.7
poly-**8**	−0.73	0.6

[a] 0.1 mol dm^{-3} *n*-Bu_4NClO_4 (for poly-**5**, *n*-Bu_4NBF_4) in PhCN, Pt electrode, scan rate 10 mV s^{-1}, V vs SCE. [b] On ITO electrode.

gave dedoped polymers.

Properties of Polymers. The resulting polymers were dark blue−green and showed relatively high stability under normal conditions. The surfaces of most of the polymers were powdery. The polymers with longer alkyl chains looked slightly smooth.

Figure 2 presents representative CVs of the polymers on Pt electrodes. Long alkyl chains did not affect the electrochemical behavior substantially. To gain reproducible clear CVs, careful conditions (especially, purification of solvents, oxygen-free atmosphere, and applied potentials on preparation) were necessary. As seen in Figure 2A, almost all the polymers exhibited redox waves in both p- and n-doping regions. The p-doping process was broad and irreversible, while the n-doping process was sharp and quasi-reversible similarly to other narrow-bandgap polymers.[42] In Figure 2A,B,F, clear prepeaks are observed. When the CVs were measured in only n-doping or p-doping region, the prepeaks did not emerge. Therefore, these peaks can be ascribed to charge trapping.[43,44] In Figures 2D and 2E, a low n-doping charge is observed in the preceding main reduction peak. This also may be indicative of charge trapping. Figure 2G shows a considerably low n-doping charge compared to other polymers, and Figure 2H shows the reduction of peak for n-doping with increasing potential cycling. These might result from the slow transport of countercation. Perhaps the effect of morphology derived from the nonplanar conformation would be associated with the n-doping process. A summary of the cathodic peak potentials for n-doping is given in Table 3. The values shift to more negative potentials than those of the corresponding monomers. While the onset potentials for p-doping are seen at around 0 V, those for n-doping vary with structure, thus chiefly depending on the *o*-quinoid-acceptor heterocycles similarly to the monomers. The differences in onset potentials between the p-doping and n-doping are smaller than the usual π-conjugated polymers. This result suggests that the polymers presented here have narrow bandgaps. In particular, Figure 2E shows a considerably narrow-bandgap polymer. The bandgap values (E_g) can be estimated from the optical absorption edge and nearly correspond to the electrochemical values. The bandgaps determined from the polymers on ITO-coated glass electrodes are shown in Table 3. These values vary from 0.5 to 1.4 eV, which are considerably small compared with usual π-conjugated polymers, confirming that they are narrow-bandgap systems. Furthermore, this finding shows that the bandgap is widely tunable by the polymer structure. In this case, the bandgaps are dependent on the electron-accepting properties of the *o*-quinoid-acceptor segments. The polymers containing **BBT** that is the strongest acceptor exhibited the narrowest bandgap. Figure 3A[45] shows the electronic spectra of the narrowest-bandgap system. The difference spectra between applied potentials and 0.0 V are shown in Figure 3B. With increasing the potentials, new absorption bands at about 0.5 and 1.7 eV appear and the peak at around 1.0 eV descends, supporting that Figure 3A shows the electronic spectra of dedoped poly-**5**.[46]

Conclusions

A series of new monomers composed of aromatic-donor and *o*-quinoid-acceptor units was prepared. The X-ray analyses revealed that some monomers containing thiophene rings have almost planar conformations. The electronic spectra and the electrochemical behavior of monomers were greatly affected by the properties of the *o*-quinoid-acceptor heterocycles. The polymers were prepared using a successive potential scan technique. Despite the presence of long alkyl chains, the polymers were insoluble. Most of the polymers exhibited both p- and n-doping processes, indicating amphoteric properties. On the other hand, the polymers composed of *N*-methylpyrrole did not show appreciable n-doping probably due to slow ion transport. The small differences between the onset potentials for p- and n-doping of the polymers imply narrow-bandgap polymers. The bandgap values determined from the absorption spectra were in the range 0.5−1.4 eV, mainly depending upon the properties of *o*-quinoid-acceptor heterocycles. The polymer possessing **BBT** showed one of the narrowest-bandgap reported so far.

Experimental Section

General Techniques. Melting points were measured on a Yanaco MP-500D or a Büchi 535 melting point apparatus and are uncorrected. IR spectra were recorded as KBr pressed pellets on a Perkin-Elmer 1640 FT-IR spectrometer. ^{1}H NMR and ^{13}C NMR spectra were recorded on a JEOL GX400 FT spectrometer at 400 and 100 MHz or on a JEOL EX270 FT spectrometer at 270 and 67.8 MHz, respectively. UV−vis−NIR spectra were recorded on a Shimadzu UV-3101PC spectrometer. Electron impact mass spectra [MS (EI)] were obtained at 70 eV on a Shimadzu QP-1000EX. The *m*/*z* values listed below are followed by relative intensities given in parentheses. Elemental analyses were carried out on a Yanaco MT-3 CHN corder. High-resolution mass determinations (HRMS) were obtained on a Shimadzu Kratos Concept 1s mass spectrometer. Column chromatography was performed on silica gel (Wakogel C-300). All reactions were performed under argon.

Computational Method. The energy levels of heterocyclic segments and geometries of monomers were calculated by using the MNDO-PM3 method in the MOPAC 6.1 program.[27] These calculations were performed with the Sony-Tektronix CAChe system.

Materials. Tetrahydrofuran (THF) and acetonitrile (MeCN) were distilled under argon from $LiAlH_4$ and CaH_2, respectively,

(42) King, G.; Higgins, S. J. *J. Mater. Chem.* **1995**, *5*, 447.
(43) Guerrero, D. J.; Ren, X.; Ferraris, J. P. *Chem. Mater.* **1994**, *6*, 1437.
(44) Zotti, G.; Schiavon, G.; Zecchin, S. *Synth. Met.* **1995**, *72*, 275.
(45) The absorption edge cannot be determined accurately because of the intense absorption of the ITO electrode itself.
(46) The electrical conductivities of compressed pellets of dedoped and I_2-doped polymers were 5.0×10^{-5} and 5.6×10^{-3} S cm^{-1}.

Table 4. Crystal Data for Compounds 1b, 2a, 4c, and 5

compd	**1b**	**2a**	**4c**	**5**
formula	$C_{16}H_{12}N_2S_3$	$C_{18}H_{14}N_2S_2$	$C_{28}H_{32}N_4S_3$	$C_{14}H_6N_4S_4$
formula wt	328.46	322.45	520.77	358.47
cryst syst	orthorhombic	monoclinic	triclinic	monoclinic
space group	$P2_12_12_1$	$P2_1/a$	$P\bar{1}$	$P2_1/n$
a, Å	5.689(1)	6.337(3)	11.717(4)	17.393(8)
b, Å	8.084(1)	20.570(3)	16.005(4)	4.818(2)
c, Å	32.842(2)	12.007(4)	7.552(3)	8.345(4)
α, deg	90.0	90.0	92.04(2)	90.0
β, deg	90.0	99.69(2)	104.46(2)	99.17(2)
γ, deg	90.0	90.0	97.63(2)	90.0
V, Å^3	1510.4(2)	1542.9(10)	1342.2(8)	690.3(6)
Z	4	4	2	2
cryst size, mm	0.35 × 0.04 × 0.03	0.45 × 0.10 × 0.05	0.45 × 0.15 × 0.10	0.25 × 0.10 × 0.05
d_{calcd}, g cm^{-3}	1.45	1.39	1.29	1.72
radiation	Cu Kα	Cu Kα	Cu Kα	Cu Kα
$2\theta_{max}$, deg	1, 70	1, 70	1, 70	1,70
obsd unique data	1477 (3σ)	1454 (3σ)	3557 (3σ)	1052 (3σ)
R	0.053	0.092	0.073	0.063
R_w	0.060	0.084	0.076	0.067

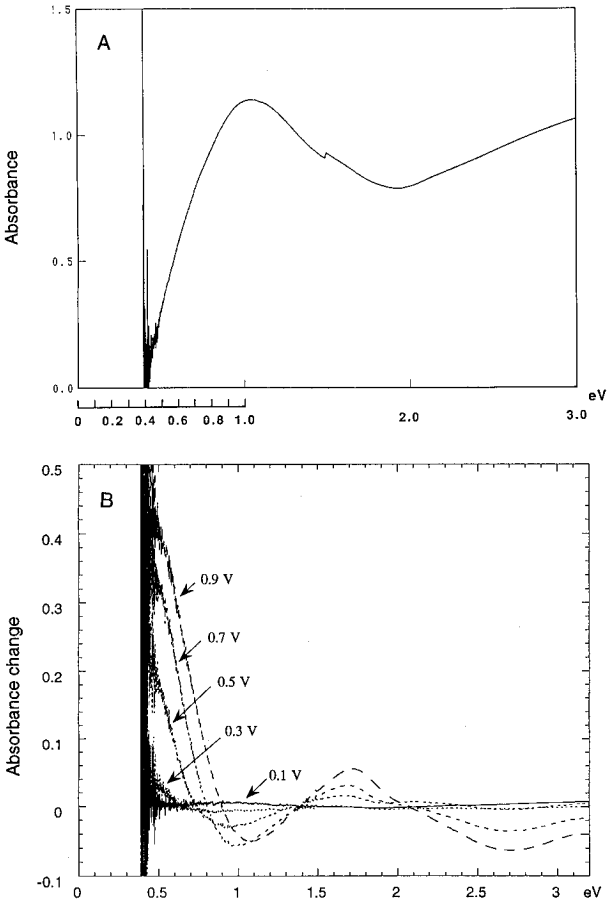

Figure 3. (A) Absorption spectrum of poly-**5** on an ITO electrode at 0.0 V. (B) The difference absorption spectra from poly-**5** at 0.0 V as a function of applied potentials in the range 0.1−0.9 V.

prior to use. Pyridine was distilled under argon from NaOH. Benzonitrile (PhCN) was purified under argon by passing through Merck aluminium oxide 90 (neutral, activity I). All other reagents and solvents purchased from Tokyo Kasei, Kanto, Wako, Aldrich, or Merck were used without further purification unless otherwise noted. 2,5-Dibromo-3,4-dinitrothiophene,[30] 7,8-tetradecanedione,[34] 14,15-octacosanedione,[35] tributyl(thien-2-yl)stannane,[31] tributyl(*N*-methylpyrrol-2-yl)stannane[39] were prepared according to literature methods. 4,7-Dibromo-5,6-dinitro-2,1,3-benzothiadiazole[38] was prepared from 4,7-dibromo-2,1,3-benzothiadiazole[37] by improved nitration.[47]

3′,4′-Diamino-2,2′:5′,2″-terthiophene (9). To a solution of 2,5-dibromo-3,4-dinitrothiophene[30] (5.01 g, 15.1 mmol) and tributyl(thien-2-yl)stannane[31] (13.47 g, 36.1 mmol) in THF (100 mL), $PdCl_2(PPh_3)_2$ (108 mg, 1 mol %) was added. The mixture was refluxed for 16 h. After cooling, the reaction mixture was concentrated under reduced pressure. To the residue hexane was added, and then the resulting yellow precipitates were filtered off, washed with hexane, and collected. Recrystallization from methanol−toluene gave the dinitro compound (2.88 g, 60%), mp 149−151 °C. Anal. Calcd for $C_{12}H_6N_2S_3O_4$: C, 42.6; H, 1.79; N, 8.28. Found: C, 42.49; H, 2.04; N, 8.15. The dinitro compound (2.88 g, 9.05 mmol) was suspended in ethanol (30 mL) and concentrated HCl (60 mL). To the mixture a solution of anhydrous $SnCl_2$ (51.19 g, 270 mmol) in EtOH (60 mL) was added. The mixture was stirred at 30 °C for 18 h and poured into a cold 25% NaOH (200 mL). Toluene (100 mL) was added to the above mixture, and then the reaction mixture was shaken vigorously and filtered through Celite. The phases were separated and the aqueous layer was extracted with toluene. The combined organic layer was washed with brine and dried over Na_2SO_4. After removal of the solvent under reduced pressure, recrystallization from ethanol afforded the title compound **9** (1.56 g, 62%) as yellowish brown needles, mp 96−96.5 °C; ^{1}H NMR (400 MHz, $CDCl_3$) δ 3.72 (s, 4H), 7.05−7.09 (m, 4H), 7.25 (dd, J = 1.5, 4.9 Hz, 2H); ^{13}C NMR (100 MHz, $CDCl_3$) δ 110.0, 123.9, 124.0, 127.7, 133.6, 135.9; IR (KBr) 3219 (NH) cm^{-1}; UV−vis ($CHCl_3$) λ_{max} 358 nm (log ϵ 4.25); MS (EI) m/z (rel intensity) 278 (M^+, 100), 127 (21). Anal. Calcd for $C_{12}H_{10}N_2S_3$: C, 51.77; H, 3.62; N, 10.06. Found: C, 51.69; H, 3.71; N, 9.93.

General Procedure for the Preparation of 2,3-Dialkyl-5,7-dithien-2-ylthieno[3,4-*b*]pyrazines (1). A mixture of 0.1−0.2 mmol of diamine **9** and 1.4 equiv of 2,3-dihydroxy-1,4-dioxane[36] (for compound **1a**) or 1.2−2 equiv of 1,2-diketones (diacetyl, 7,8-tetradecanedione,[34] and 14,15-octacosanedione[35] for compounds **1b**−**d**, respectively) was stirred at 60 °C in MeOH (5−10 mL) for 1 h. After removal of the solvent under reduced pressure, the crude product was purified by column chromatography and recrystallization.

1a: yield 52%; reddish purple needles; mp 179−179.5 °C (from hexane); ^{1}H NMR (400 MHz, $CDCl_3$) δ 7.12 (dd, J = 3.7, 5.2 Hz, 2H), 7.40 (dd, J = 0.9, 5.2 Hz, 2H), 7.63 (dd, J = 0.9, 3.7 Hz, 2H), 8.50 (s, 2H); ^{13}C NMR (100 MHz, $CDCl_3$) δ 118.1, 118.7, 119.8, 120.4, 127.0, 132.1, 137.3; UV−vis ($CHCl_3$) λ_{max} 532 nm (log ϵ 3.93); MS (EI) m/z (rel intensity) 300 (M^+, 100). Anal. Calcd for $C_{14}H_8N_2S_3$: C, 55.97; H, 2.68; N, 9.32. Found: C, 55.75; H, 2.98; N, 9.16.

1b: yield 82%; red needles; mp 210−211 °C (from ethanol−toluene); ^{1}H NMR (400 MHz, $CDCl_3$) δ 2.67 (s, 6H), 7.11 (dd, J = 3.7, 5.2 Hz, 2H), 7.36 (dd, J = 1.2, 5.2 Hz, 2H), 7.63 (dd, J = 1.2, 3.7 Hz, 2H); ^{13}C NMR (100 MHz, $CDCl_3$) δ 23.7, 123.7,

(47) Coon, C. L.; Blucher, W. G.; Hill, M. E. *J. Org. Chem.* **1973**, *38*, 4243.

124.4, 126.0, 127.2, 134.7, 138.0, 153.4; UV−vis ($CHCl_3$) λ_{max} 500 nm (log ϵ 3.99); MS (EI) *m/z* (rel intensity) 328 (M^+, 100), 202 (18), 101 (21). Anal. Calcd for $C_{16}H_{12}N_2S_3$: C, 58.50; H, 3.68; N, 8.53. Found: C, 58.42; H, 3.78; N, 8.61.

1c: yield 85%; red fibers; mp 116−116.5 °C (from ethanol); ^{1}H NMR (400 MHz, $CDCl_3$) δ 0.89 (t, J = 7.0 Hz, 6H), 1.21−1.41 (m, 12H), 1.47 (dd, J = 6.7, 7.0 Hz, 4H), 2.14 (t, J = 7.0 Hz, 4H), 7.10 (dd, J = 3.7, 5.2 Hz, 2H), 7.36 (dd, J = 1.2, 5.2 Hz, 2H), 7.61 (dd, J = 1.2, 3.7 Hz, 2H); ^{13}C NMR (100 MHz, $CDCl_3$) δ 14.2, 22.7, 26.7, 29.1, 31.9, 35.0, 123.5, 123.8, 126.0, 127.0, 135.0, 137.6, 156.2; UV−vis ($CHCl_3$) λ_{max} 502 nm (log ϵ 4.01); MS (EI) *m/z* (rel intensity) 468 (M^+, 100), 398 (34), 355 (28), 328 (29). Anal. Calcd for $C_{26}H_{32}N_2S_3$: C, 66.62; H, 6.88; N, 5.98. Found: C, 66.67; H, 6.87; N, 6.14.

1d: yield 75%; red solid; mp 65−67 °C (from ethanol−toluene); ^{1}H NMR (400 MHz, $CDCl_3$) δ 0.88 (t, J = 6.7 Hz, 6H), 1.20−1.53 (m, 40H), 1.93 (quintet, J = 7.3 Hz, 4H), 2.85 (t, J = 7.3 Hz, 4H), 7.06 (dd, J = 3.7, 5.2 Hz, 2H), 7.32 (dd, J = 0.9, 5.2 Hz, 2H), 7.56 (dd, J = 0.9, 3.7 Hz, 2H); ^{13}C NMR (100 MHz, $CDCl_3$) δ 14.1, 22.7, 26.7, 29.4, 29.6, 29.7 (6CH_2), 31.9, 35.0, 123.5, 123.8, 126.0, 127.0, 135.0, 137.6, 156.2; UV−vis ($CHCl_3$) λ_{max} 500 nm (log ϵ 4.01); MS (EI) *m/z* (rel intensity) 664 (M^+, 100), 496 (22), 329 (23). Anal. Calcd for $C_{40}H_{60}N_2S_3$: C, 72.23; H, 9.09; N, 4.21. Found: C, 72.30; H, 8.89; N, 4.07.

4,7-Dithien-2-yl-2,1,3-benzothiadiazole (3). To a solution of 4,7-dibromo-2,1,3-benzothiadiazole[37] (4.05 g, 15.0 mmol) and tributyl(thien-2-yl)stannane[31] (13.47 g, 36.1 mmol) in THF (100 mL), $PdCl_2(PPh_3)_2$ (213 mg, 2 mol %) was added. The mixture was refluxed for 3 h. After removal of the solvent under reduced pressure, the residue was purified by column chromatography on silica gel (eluent CH_2Cl_2/hexane, 1:1). Recrystallization from ethanol−toluene gave the title compound **2** (3.70 g, 82%) as red needles, mp 121−123 °C; ^{1}H NMR (400 MHz, $CDCl_3$) δ 7.21 (dd, J = 3.7, 4.9 Hz, 2H), 7.45 (dd, J = 0.9, 4.9 Hz, 2H), 7.86 (s, 2H), 8.11 (dd, J = 0.9, 3.7 Hz, 2H); ^{13}C NMR (100 MHz, $CDCl_3$) δ 125.8, 126.0, 126.8, 127.5, 128.0, 139.3, 152.6; UV−vis ($CHCl_3$) λ_{max} 446 nm (log ϵ 4.11); MS (EI) *m/z* (rel intensity) 300 (M^+, 100). Anal. Calcd for $C_{14}H_8N_2S_3$: C, 55.97; H, 2.68; N, 9.32. Found: C, 56.10; H, 2.87; N, 9.31.

1,2-Diamino-3,6-dithien-2-ylbenzene (10). A mixture of **2** (300 mg, 1.00 mmol) and zinc dust (1.33 g, 20.3 mmol) in acetic acid (15 mL) was refluxed for 15 min. The reaction mixture was filtered and the residue was washed with Et_2O. Et_2O (100 mL) was added to the filtrate and the solution was washed with 5% NaOH and brine. The organic layer was dried over $MgSO_4$. After removal of the solvent under reduced pressure, purification by column chromatography on silica gel (eluent CH_2Cl_2) afforded the title compound **10** (257 mg, 94%) as a pink solid, mp 109−109.5 °C (from ethanol); ^{1}H NMR (400 MHz, $CDCl_3$) δ 3.86 (brs, 4H), 6.87 (s, 2H), 7.13 (dd, J = 3.7, 5.2 Hz, 2H), 7.18 (dd, J = 0.9, 3.7 Hz, 2H), 7.36 (dd, J = 0.9, 5.2 Hz, 2H); ^{13}C NMR (100 MHz, $CDCl_3$) δ 114.0, 114.4, 118.5, 119.0, 120.5, 126.0, 134.0; IR (KBr) 3388 (NH) cm^{-1}; UV−vis ($CHCl_3$) λ_{max} 297 nm (log ϵ 4.19); MS (EI) *m/z* (rel intensity) 272 (M^+, 100), 227 (33). Anal. Calcd for $C_{14}H_{12}N_2S_2$: C, 61.73; H, 4.44; N, 10.28. Found: C, 61.59; H, 4.46; N, 10.22.

General Procedure for the Preparation of 2,3-Dialkyl-5,8-dithien-2-ylquinoxalines (2). A mixture of diamine **10** (100 mg, 0.37 mmol) and 1.0−1.5 equiv of 1,2-diketones (diacetyl and 7,8-tetradecanedione[34] for compounds **2a** and **2b**, respectively) in acetic acid (5 mL) was stirred at room temperature for 10 min. After removal of the solvent under reduced pressure, the residue was purified by column chromatography and recrystallization.

2a: yield 89%; yellow needles; mp 237−238 °C (from ethanol); ^{1}H NMR (400 MHz, $CDCl_3$) δ 2.81 (s, 6H), 7.17 (dd, J = 3.7, 5.7 Hz, 2H), 7.48 (dd, J = 0.6, 5.2 Hz, 2H), 7.85 (dd, J = 0.6, 3.7 Hz, 2H), 8.03 (s, 2H); ^{13}C NMR (100 MHz, $CDCl_3$) δ 15.7, 119.2, 119.4, 119.6, 121.3, 123.9, 130.5, 132.1, 145.3; UV−vis ($CHCl_3$) λ_{max} 405 nm (log ϵ 4.12); MS (EI) *m/z* (rel intensity) 322 (M^+, 100), 307 (36). Anal. Calcd for $C_{18}H_{14}N_2S_2$: C, 67.05; H, 4.38; N, 8.69. Found: C, 66.09; H, 4.59; N, 8.62.

2b: yield 90%; yellow fibers; mp 125−126 °C (from ethanol); ^{1}H NMR (400 MHz, $CDCl_3$) δ 0.91 (t, J = 7.5 Hz, 6H), 1.31−1.46 (m, 12H), 2.03 (quintet, J = 7.6 Hz, 4H), 3.09 (t, J = 7.6 Hz, 4H), 7.17 (dd, J = 3.6, 4.9 Hz, 2H), 7.49 (d, J = 4.9 Hz, 2H), 7.84 (d, J = 3.6 Hz, 2H), 8.05 (s, 2H); ^{13}C NMR (100 MHz, $CDCl_3$) δ 7.1, 15.6, 20.9, 22.3, 24.8, 28.0, 119.0, 119.1, 119.4, 121.3, 123.9, 130.3, 132.1, 148.4; UV−vis ($CHCl_3$) λ_{max} 407 nm (log ϵ 4.10); MS (EI) *m/z* (rel intensity) 462 (M^+, 59), 392 (100), 322 (64). Anal. Calcd for $C_{28}H_{34}N_2S_2$: C, 72.68; H, 7.41; N, 6.05. Found: C, 72.46; H, 7.33; N, 6.06.

5,6-Dinitro-4,7-dithien-2-yl-2,1,3-benzothiadiazole (11). To a solution of 4,7-dibromo-5,6-dinitro-2,1,3-benzothiadiazole[38] (3.80 g, 9.9 mmol) and tributyl(thien-2-yl)stannane[31] (8.51 g, 22.8 mmol) in THF (30 mL), $PdCl_2(PPh_3)_2$ (143 mg, 2 mol %) was added. The mixture was refluxed for 3 h. After cooling, an orange solid appeared. The solid was filtered off, washed with MeCN, and collected. Recrystallization from THF gave the title compound **11** (1.82 g, 47%) as an orange solid, mp 259−260 °C; ^{1}H NMR (270 MHz, $CDCl_3$) δ 7.23 (dd, J = 3.6, 5.3 Hz, 2H), 7.52 (dd, J = 1.2, 3.6 Hz, 2H), 7.74 (dd, J = 1.2, 5.3 Hz, 2H); UV−vis ($CHCl_3$) λ_{max} 428 nm (log ϵ 4.02); MS (EI) *m/z* (rel intensity) 390 (M^+, 100), 285 (56), 221 (50), 133 (63), 127 (52). Anal. Calcd for $C_{14}H_6N_4O_4S_3$: C, 43.07; H, 1.55; N, 14.35. Found: C, 43.06; H, 1.84; N, 14.05.

5,6-Diamino-4,7-dithien-2-yl-2,1,3-benzothiadiazole (12). A mixture of dinitro compound **11** (780 mg, 2.0 mmol) and iron dust (1.33 g, 24.0 mmol) in acetic acid (40 mL) was stirred at 30 °C for 4 h. The reaction mixture was poured into cold 5% NaOH (50 mL), and then a yellow solid appeared. The solution was extracted with Et_2O. The organic layer was washed with brine and dried over Na_2SO_4. After removal of the solvent under reduced pressure, the residue was purified by column chromatography on silica gel (eluent CH_2Cl_2). Recrystallization from $CHCl_3$ gave the title compound **12** (383 mg, 58%) as yellow plates, mp 240−242 °C; IR (KBr) 3298 (NH) cm^{-1}; ^{1}H NMR (400 MHz, $CDCl_3$) δ 4.39 (s, 4H), 7.25 (dd, J = 3.7, 5.2 Hz, 2H), 7.36 (dd, J = 1.2, 3.7 Hz, 2H), 7.55 (dd, J = 1.2, 5.2 Hz, 2H); ^{13}C NMR (100 MHz, $CDCl_3$) δ 100.1, 120.2, 120.4, 121.5, 128.2, 132.3, 143.9; UV−vis ($CHCl_3$) λ_{max} 362 nm (log ϵ 4.20); MS (EI) *m/z* (rel intensity) 330 (M^+, 100), 285 (21), 264 (16). Anal. Calcd for $C_{14}H_{10}N_4S_3$: C, 50.89; H, 3.05; N, 16.96. Found: C, 50.79; H, 3.11; N, 16.90.

General Procedure for the Preparation of 6,7-Dialkyl-4,9-dithien-2-yl[1,2,5]thiadiazolo[3,4-*g*]quinoxalines (4). A mixture of 0.1−0.2 mmol of diamine **12** and 1.4 equiv of 2,3-dihydroxy-1,4-dioxane[36] (for compound **4a**) or 1.6−2.0 equiv of 1,2-diketones (diacetyl and 7,8-tetradecanedione[34] for compound **4b** and **4c**, respectively) was stirred at room temperature for 10 min. After removal of the solvent under reduced pressure, the residue was purified by column chromatography and recrystallization.

4a: yield 50%; blue solid; mp 253−255 °C (from ethanol−toluene); ^{1}H NMR (270 MHz, $CDCl_3$) δ 7.32 (dd, J = 4.0, 5.0 Hz, 2H), 7.70 (dd, J = 1.0, 5.0 Hz, 2H), 8.87 (dd, J = 1.0, 4.0 Hz, 2H), 8.98 (s, 2H); UV−vis ($CHCl_3$) λ_{max} 606 nm (log ϵ 4.01); MS (EI) *m/z* (rel intensity) 352 (M^+, 100), 307 (23). Anal. Calcd for $C_{16}H_8N_4S_3$: C, 54.53; H, 2.29; N, 15.90. Found: C, 54.79; H, 2.58; N, 15.79.

4b: yield 82%; blue needles; mp 257−259 °C (from ethanol−toluene); ^{1}H NMR (400 MHz, $CDCl_3$) δ 2.83 (s, 6H), 7.30 (dd, J = 4.0, 5.0 Hz, 2H), 7.64 (dd J = 0.6, 5.2 Hz, 2H), 8.98 (dd, J = 0.6, 4.0 Hz, 2H); UV−vis ($CHCl_3$) λ_{max} 591 nm (log ϵ 4.06); MS (EI) *m/z* (rel intensity) 380 (M^+, 100), 365 (40), 347 (34). Anal. Calcd for $C_{28}H_{32}N_4S_3$: C, 64.15; H, 4.85; N, 22.44. Found: C, 64.19; H, 5.10; N, 22.43.

4c: yield 75%; blue needles; mp 114−115 °C (from ethanol); ^{1}H NMR (400 MHz, $CDCl_3$) δ 0.92 (t, J = 7.3 Hz, 6H), 1.35−1.58 (m, 12H), 2.07 (quintet, J = 7.6 Hz, 4H), 3.14 (t, J = 7.6 Hz, 4H), 7.31 (dd, J = 4.0, 5.2 Hz, 2H), 7.65 (dd J = 0.6, 5.2 Hz, 2H), 8.98 (dd, J = 0.6, 4.0 Hz, 2H); ^{13}C NMR (100 MHz, $CDCl_3$) δ 14.1, 22.6, 27.9, 29.3, 31.8, 35.4, 126.5, 130.6, 132.6, 135.1, 135.8, 151.4, 152.8, 157.3; UV−vis ($CHCl_3$) λ_{max} 593 nm (log ϵ 4.07); MS (EI) *m/z* (rel intensity) 520 (M^+, 100), 450 (51), 435 (26), 381 (44). Anal. Calcd for $C_{28}H_{32}N_4S_3$: C, 64.58; H, 6.19; N, 10.76. Found: C, 64.52; H, 6.08; N, 10.60.

4,8-Dithien-2-yl-2$\lambda^4\delta^2$-benzo[1,2-*c*;4,5-*c*′]bis[1,2,5]-thiadiazole (5). A mixture of diamine **12** (996 mg, 3.0 mmol), *N*-sulfinylaniline (848 mg, 6.0 mmol), and chlorotrimethylsi-

lane (592 mg, 5.4 mmol) in pyridine (15 mL) was stirred at 80 °C for 24 h. To the reaction solution tetrachloromethane (50 mL) was added, and the resulting solid was filtered off and collected. The solid was sublimed at 300 °C/0.05 Torr to give blue crystals of **5** (880 mg, 82%), mp 334−336 °C; UV−vis ($CHCl_3$) λ_{max} 702 nm (log ϵ 4.07); MS (EI) *m*/*z* (rel intensity) 358 (M^+, 100), 147 (16). Anal. Calcd for $C_{14}H_6N_4S_4$: C, 46.92; H, 1.69; N, 15.65. Found: C, 47.18; H, 1.99; N, 15.73.

5,6-Diamino-4,7-bis(*N*-methylpyrrol-2-yl)-2,1,3-benzothiadiazole (14). According to the same procedures for the preparation of **11** and **13**, the reaction with 4,7-dibromo-5,6-dinitro-2,1,3-benzothiadiazole[38] (2.69 g, 7.0 mmol), tributyl(*N*-methylpyrrol-2-yl)stannane[39] (5.75 g, 15.5 mmol), $PdCl_2(PPh_3)_2$ (98 mg, 2 mol %), and THF (20 mL) afforded the title compound **14** (1.66 g, 73%) as a yellow solid, mp 186 °C (dec); ^{1}H NMR (400 MHz, $CDCl_3$) δ 3.46 (s, 4H, NCH_2H), 3.47 (s, 2H, NCH_2H), 4.29 (s, 4H), 6.33−6.36 (m, 4H), 6.88 (dd, J = 1.8, 2.1 Hz, 2H); ^{13}C NMR (100 MHz, $CDCl_3$) δ 34.9, 105.6, 108.3, 110.0, 123.8, 125.5, 140.7, 151.3; IR (KBr) 3322 (NH) cm^{-1}; UV−vis ($CHCl_3$) λ_{max} 364 nm (log ϵ 4.14); MS (EI) *m*/*z* (rel intensity) 324 (M^+, 100), 282 (21); HRMS (EI) Calcd for $C_{16}H_{16}N_6S$: 324.1157. Found 324.1159.

6,7-Dialkyl-4,9-bis(*N*-methylpyrrol-2-yl)[1,2,5]thiadiazolo[3,4-*g*]quinoxalines (7). According to the same procedure for the preparation of **4**, the title compounds **7** were synthesized from diamine **14** and 1,2-diketones (diacetyl and 7,8-tetradecanedione[34] for compound **7a** and **7b**, respectively).

7a: yield 62%; bluish purple solid; mp 221−223 °C (dec) (from ethanol); ^{1}H NMR (400 MHz, $CDCl_3$) δ 2.72 (s, 6H), 3.57 (s, 6H), 6.47 (dd, J = 2.1, 3.7 Hz, 2H), 6.66 (dd, J = 1.8, 3.7 Hz, 2H), 6.98 (dd, J = 1.8, 2.1 Hz, 2H); ^{13}C NMR (100 MHz, $CDCl_3$) δ 23.8, 36.1, 108.5, 114.2, 121.6, 124.9, 127.5, 137.2, 153.5, 154.9; UV−vis ($CHCl_3$) λ_{max} 572 nm (log ϵ 3.90); MS (EI) *m*/*z* (rel intensity) 374 (M^+, 100), 332 (28). Anal. Calcd for $C_{20}H_{18}N_6S$: C, 64.15; H, 4.85; N, 22.44. Found: C, 64.19; H, 5.10; N, 22.43.

7b: yield 59%; bluish purple solid; mp 109−110 °C (from ethanol); ^{1}H NMR (400 MHz, $CDCl_3$) δ 0.90 (t, J = 7.0 Hz, 6H), 1.27−1.49 (m, 12H), 1.82 (quintet, J = 7.6 Hz, 4H), 2.97 (t, J = 7.6 Hz, 4H), 3.56 (s, 6H), 6.45 (dd, J = 2.1, 3.6 Hz, 2H), 6.63 (dd, J = 1.5, 3.6 Hz, 2H), 6.97 (dd, J = 1.8, 2.1 Hz, 2H); ^{13}C NMR (100 MHz, $CDCl_3$) δ 14.1, 22.6, 27.4, 29.3, 31.7, 35.5, 36.0, 108.4, 114.0, 121.6, 124.5, 127.5, 137.6, 153.5, 157.9; UV−vis ($CHCl_3$) λ_{max} 571 nm (log ϵ 3.90); MS (EI) *m*/*z* (rel intensity) 514 (M^+, 88), 444 (21), 280 (30), 107 (100). Anal. Calcd for $C_{28}H_{32}N_4S_3$: C, 70.00; H, 7.44; N, 16.33. Found: C, 70.28; H, 7.37; N, 16.19.

4,8-Bis(*N*-methylpyrrol-2-yl)-2$\lambda^4\delta^2$-benzo[1,2-c;4,5-c′]bis[1,2,5]thiadiazole (8). According to the same procedure for the preparation of **5**, the title compound **8** was synthesized from diamine **14**: yield 28%; blue solid; mp 279−280 °C (from toluene−CH_2Cl_2); ^{1}H NMR (400 MHz, $CDCl_3$) δ 3.72 (s, 6H), 6.47 (dd, J = 2.7, 4.0 Hz, 2H), 6.83 (dd, J = 1.8, 4.0 Hz, 2H), 7.02 (dd, J = 1.8, 2.7 Hz, 2H); ^{13}C NMR (100 MHz, $CDCl_3$) δ 36.5, 109.5, 113.2, 115.5, 126.5, 126.6, 127.9, 153.0; UV−vis ($CHCl_3$) λ_{max} 694 nm (log ϵ 4.06); MS (EI) *m*/*z* (rel intensity) 352 (M^+, 100). Anal. Calcd for $C_{16}H_{12}N_6S_2$: C, 54.53; H, 3.43; N, 23.85. Found; C, 54.42; H, 3.64; 23.64.

2,3,7,8-Tetramethyl-5,10-dithien-2-ylpyrazino[2,3-*g*]quinoxaline (6). A mixture of dinitrobenzothiadiazole **11** (197 mg, 0.51 mmol) and zinc dust (693 mg, 10.6 mmol) in acetic acid (5 mL) was stirred at 60 °C for 1 h until the reaction mixture turned white. After this was cooled to room temperature, diacetyl (0.35 g, 4.1 mmol) was added to the solution and the mixture was stirred for 1 h. After removal of the solvent under reduced pressure, the residue was purified by column chromatography on silica gel (eluent CH_2Cl_2). Recrystallization from THF gave the title compound **6** (108 mg, 53%) as a red solid, mp 175−176 °C (dec); ^{1}H NMR (270 MHz, $CDCl_3$) δ 5.23 (s, 12H), 7.29 (dd, J = 4.0, 5.3 Hz, 2H), 7.65 (dd, J = 1.0, 5.3 Hz, 2H), 8.38 (dd, J = 1.0, 4.0 Hz, 2H); UV−vis ($CHCl_3$) λ_{max} 491 nm (log ϵ 3.96); MS (EI) *m*/*z* (rel intensity) 402 (M^+, 100), 387 (38), 369 (33). Anal. Calcd for $C_{22}H_{18}N_4S_2$: C, 65.65; H, 4.51; N, 13.92. Found; C, 65.71; H, 4.57; N 13.82.

X-ray Structure Analyses. The crystals for the data collections were prepared by slow evaporation of the solvents used for recrystallization (chloroform for **1b**, hexane for **2a**, ethanol/hexane for **4c**, and carbon tetrachloride for **5**). An Enraf-Nonius CAD4 diffractometer was used with graphite-monochromated Cu Kα radiation, $\theta/2\theta$ scan technique. The crystal data are summarized in Table 4. Cell parameters were determined from least-squares procedures on 25 reflections (44° < 2θ < 50°). No significant variation was observed in intensities of three standards monitored every 7200 s. The structures were solved by the direct method using the MULTAN78[48] or SHELXS86[49] program and refined by the block-diagonal least-squares analysis based on F values using UNICS III program package.[50] Thiophene rings were statistically disordered by the 180° rotation in the crystal. New ideal atoms of X [S α% and C (100 − α)%] and Y [S (100 − α)% and C α%] were prepared from mixed atom scattering factors and applied at the disorder positions. All the non-hydrogen atoms of the molecule were refined with anisotropic temperatures factors. At the final stage, hydrogen atoms were included in the refinement with isotropic temperature factors. These calculations were carried out in the Computer Center of Institute for Molecular Science.[51]

Electrochemistry. Cyclic voltammetry of monomers was carried out with a Toho Technical Research Polarization Unit PS-07 potentiostat/galvanostat in a three-compartment cell in PhCN or MeCN containing 0.1 mol dm^{-3} *n*-Bu_4NClO_4 at a scan rate of 100 mV s^{-1}. Solutions were degassed by argon bubbling before use, and an argon stream was maintained over the solutions during measurements. Pt disk (2.0 mm^{-2}), Pt wire, and SCE were used as the working, counter, and reference electrodes, respectively. Cyclic voltammetry of the polymers was performed in monomer-free electrolytes at 10 mV s^{-1} under the same conditions as that of the monomers.

General Procedure for Electrochemical Polymerization. Polymers were prepared by a cyclic potential sweep technique (−0.5−0 to 0.9−1.2 V) with 0.5−2 mmol dm^{-3} monomer solutions under the same conditions described above. For measurements of UV−vis−NIR spectra, the polymers were deposited on an ITO glass electrode. Dedoping was performed by electrochemical reduction of self-standing, doped polymer films in monomer-free electrolytes at potentials that do not cause doping.

Acknowledgment. We thank Dr. Michinori Karikomi of Utsunomiya University for the preparation of oligomers **3**, **4a**,**b**, and **5**. This work was supported by research fellowships from the Japan Society for the Promotion of Science for Young Science, and a Grant-in Aid of Scientific Research from the Ministry of Education, Science, Sports and Culture, Japan.

Supporting Information Available: Details of X-ray structural analysis for **2b** (15 pages). Ordering information is given on any current masthead page.

CM950467M

(48) Main, P.; Hull, S. E.; Lessinger, L.; Germain, G.; Declercq, J.-P.; Woolfson, M. M. MULTAN78, A System of Computer Programs for the Automatic Solution of Crystal Structures from X-ray Diffraction Data, Universities of York, England and Louvain, Belgium, 1978.

(49) Sheldrick, G. M. SHELXS86, Program for Crystal Structure Solution, University of Goettingen, Germany, 1986.

(50) Sakurai, T.; Kobayashi, K. *Rikagaku Kenkyusho Hokoku*, **1979**, *55*, 69.

(51) The authors have deposited atomic coordinate for **1b** and **5** with the Cambridge Crystallographic Data Centre. The coordinates can be obtained, on request, from the Director, Cambridge Crystallographic Data Centre, 12 Union Road, Cambridge, CB2 1EZ, UK.